Polarization spectra of Rb atoms and their application in laser frequency stabilization

Kaijun Jiang (江开军), Jin Wang (王 谨), Xianhua Tu (涂鲜花), Ming He (何 明), and Mingsheng Zhan (詹明生)

State Key Laboratory of Magnetic Resonance and Atomic and Molecular Physics, Wuhan Institute of Physics and Mathematics, Chinese Academy of Sciences, Wuhan 430071

Received January 21, 2003

Polarization spectra of rubidium atoms were investigated with different uncrossed angles between the polarizer and the analyzer. The variation of the spectra was derived theoretically as a function of arbitrary angle, and measured experimentally for different angles. The spectral profile of D_2 line of rubidium was further used to stabilize the frequency of a diode laser. It was demonstrated that the laser linewidth was reduced to 2 MHz.

OCIS codes: 020.0020, 140.0140, 300.0300.

Polarization spectroscopy (PS)[1], as well as saturation absorption spectroscopy (SAS)[2], is a useful Doppler-free spectroscopy method usually used for laser frequency stabilization. In saturation absorption spectra there is normally a Doppler-broadened background due to the linear absorption, while in polarization spectra this background can be greatly eliminated, which gives a better signal-to-noise ratio. Meanwhile, PS has higher relative sensitivity than SAS. Spectral profile in polarization spectra varies with the uncrossed angle (θ) between the polarizer and the analyzer that are set perpendicularly in experiments. Theoretical and experimental results of polarization spectra with small θ have been reported extensively, one example is for Na atom[3,4]. But to our knowledge, there is not experimental demonstration of polarization spectra with bigger arbitrary uncrossed angle yet. To compare different spectroscopic techniques in stabilizing laser frequency for laser cooling and trapping neutral atoms, we found that larger θ often provides better profile.

In this letter, we report the qualitative theoretical analysis and experimental study of polarization spectra of rubidium atoms with arbitrary angle. In the application of laser frequency stabilization, polarization spectrum has a good dispersion line shape that can be used directly as an error signal for feedback to the laser. Thus, polarization spectrum offers a more convenient and easier method for frequency stabilization than SAS method[5]. We have used this method to narrow the frequency of our diode laser.

Figure 1(a) is the level scheme typically for an alkali atom. Figure 1(b) is an experimental arrangement typically for the PS. There are two laser beams in the configuration of PS. A weak linearly polarized probe beam passes through atomic vapor cell and an intense circularly polarized pumping beam passes through the cell from the opposite direction and is overlapped with the probe beam. Both beams are taken from the same laser. The quantum numbers of linearly and circularly polarized light are 0,±1, respectively. So the corresponding transitions obey the selection rules $\Delta M = 0, \pm 1$. For $\Delta M = +1$ transition as shown in Fig. 1(a), even with the same pumping intensity I, due to M dependence of the absorption cross section $\sigma(F, M \rightarrow F', M')$ and different relaxation processes, the depletions of sublevels ($M = -2, -1, 0, 1, 2$) are different. This means that the population of the sublevels of the ground state is not uniform, and the orientation of the angular momentum vector F will be anisotropic for a medium after pumping. Thus, the atomic sample becomes birefringent for the linearly polarized probe beam.

The amplitude of linearly polarized probe wave can be expressed as

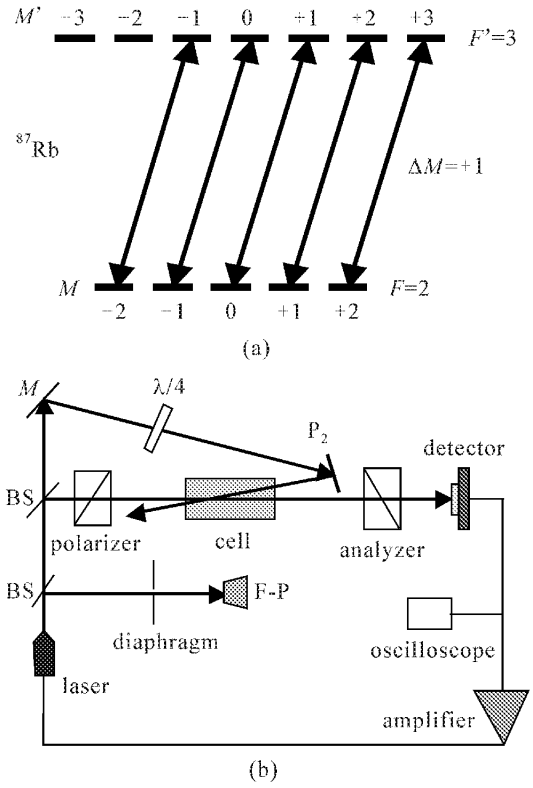

Fig. 1. Polarization spectroscopy. (a) The level scheme for a transition $F = 2 \rightarrow F = 3$; (b) experimental setup.

$$E = E_0 e^{i(\omega t - kz)}; E_0 = (E_{0x}, 0, 0). \quad (1)$$

Usually, a linearly polarized wave can be decomposed into a σ^+ and a σ^- circularly polarized components

$$E^+ = E_0^+ e^{i(\omega t - k^+ z)}; E_0^+ = \frac{1}{2} E_0 (\hat{x} + i\hat{y}),$$

$$E^- = E_0^- e^{i(\omega t - k^- z)}; E_0^- = \frac{1}{2} E_0 (\hat{x} - i\hat{y}), \quad (2)$$

where $\hat{x}$ and $\hat{y}$ are unit vectors. Due to the circularly polarized pump light, these two components have different absorption coefficients α^+ and α^-, and different refractive indices n^+ and n^- when they pass through the atomic sample. Supposing the absorption path length is L, the amplitude of two components E^- and E^+ are

$$E^- = E_0^- e^{i[\omega t - k^- z + i(\alpha^-/2)/L]},$$

$$E^+ = E_0^+ e^{i[\omega t - k^+ z + i(\alpha^+/2)/L]}. \quad (3)$$

The phase difference $\Delta\phi$ and the amplitude difference ΔE induced by the differences $\Delta\alpha = \alpha^+ - \alpha^-$ and $\Delta n = n^+ - n^-$ can be expressed as

$$\Delta\phi = (k^+ - k^-)L = (\omega L/c)(n^+ - n^-),$$

$$\Delta E = \frac{E_0}{2}[e^{-(\alpha^+/2)L} - e^{-(\alpha^-/2)L}].$$

The windows of the absorption cell also show a pressure-induced birefringence, due to the atmospheric pressure onto one side and vacuum on the other side. The additional refraction index and the absorption coefficient can be expressed as

$$n^\pm = b_r^\pm + i b_i^\pm.$$

The compositive amplitude of the σ^+ and the σ^- components is

$$E(z = L) = E^+ + E^-$$

$$= \frac{E_0}{2} e^{i\omega t} e^{-i[\omega(nL + b_r)/c - i\alpha L/2 - i b_i]}$$

$$\times [(\hat{x} + i\hat{y}) e^{-i\Delta} + (\hat{x} - i\hat{y}) e^{+i\Delta}], \quad (4)$$

where

$$n = \frac{1}{2}(n^+ + n^-); \alpha = \frac{1}{2}(\alpha^+ + \alpha^-); b = \frac{1}{2}(b^+ + b^-),$$

$$\Delta n = (n^+ - n^-); \Delta\alpha = (\alpha^+ - \alpha^-); \Delta b = (b^+ - b^-),$$

$$\Delta = \omega(L\Delta n + \Delta b_r)/2c - i(L\Delta\alpha/4 + \Delta b_i/2).$$

When the probe wave passes through the analyzer P_2, the amplitude E_t is composed of components E_x and E_y (Fig. 2),

$$E_t = E_x \sin\theta + E_y \cos\theta.$$

Generally,

$$L\Delta\alpha \ll 1, L\Delta k \ll 1, \Delta b \ll 1,$$

$$E_t \approx E_0 e^{i\omega t} e^{-i[\omega(nL + b_r)/c - i\alpha L/2 + i b_i]}$$

$$\times [\sin\theta - \Delta\cos\theta]. \quad (5)$$

The detector signal $S(\omega)$ is proportional to the transmitted intensity $I_t(\omega)$

$$S(\omega) \propto I_t(\omega) = E_t E_t^*,$$

$$I_t(\omega) = I_0 e^{-\alpha L - 2b_i} \left[\xi + \left(\sin\theta + \frac{\omega}{2c}\Delta b_r \cos\theta\right)^2 \right.$$

$$+ \cos^2\theta \left(\frac{\Delta b_i}{2}\right)^2 + \left(\sin\theta\cos\theta + \frac{\omega}{2c}\Delta b_r \cos^2\theta\right)\frac{\omega}{c} L\Delta n$$

$$\left. + \cos^2\theta \frac{L\Delta\alpha\Delta b_i}{4} + \cos^2\left(\frac{\Delta\alpha}{4}\right)^2 + \left(\frac{\omega}{c}\cos\theta L\Delta n\right)^2\right]. \quad (6)$$

In the case of

$$\Delta\alpha(\omega) = \frac{\Delta\alpha(\omega_0)}{1 + x^2}, x = \frac{\omega_0 - \omega}{\gamma_s/2},$$

where γ_s is the homogeneous linewidth induced by the pump wave. From Kramers-Kronig dispersion relation[6], we have

$$\Delta n(\omega) = \frac{c}{\omega_0}\frac{\Delta\alpha(\omega_0)x}{1 + x^2}, x = \frac{\omega_0 - \omega}{\gamma_s/2}.$$

Insert Δa and Δn into Eq. (6), the probe intensity $I_t(w)$ becomes

$$I_t(\omega) = I_0 e^{-\alpha L - 2b_i} \left\{\xi + \left(\sin\theta + \frac{\omega}{2c}\Delta b_r \cos\theta\right)^2 \right.$$

$$+ \cos^2\theta \left(\frac{\Delta b_i}{2}\right)^2 + \left(\sin\theta\cos\theta + \frac{\omega}{2c}\Delta b_r \cos^2\theta\right)\frac{L\Delta\alpha_0 x}{1 + x^2}$$

$$+ \left[\frac{L\Delta\alpha_0\Delta b_i}{4} + \left(\frac{\Delta\alpha_0}{4}\right)^2\right]\frac{\cos^2\theta}{1 + x^2}$$

$$\left. + \left(\frac{L\Delta\alpha_0\cos\theta}{2}\right)^2 \left(\frac{x}{1 + x^2}\right)^2\right\}, \quad (7)$$

where ξ is residual intensity with zero uncrossed angle, $(\sin\theta + (\omega/2c)\Delta b_r \cos\theta)^2 + \cos 2\theta(\Delta b_i/2)^2$ is the additional transmitted intensity and the absorption part due to the birefringence of windows. The next two terms contribute to Lorentzian and dispersion line shape, respectively. In most cases, $L\Delta\alpha_0 \ll 1$, we can ignore the quadratic terms, thus the spectral profiles mainly depend on $\sin\theta\cos\theta$. When $\theta = 0$, the probe signal is very weak. When θ changes from 0 to about $\pi/4$, the dispersion profile will increase. When θ changes from $\pi/4$ to $\pi/2$, the dispersion profile becomes weaker and the Lorentzian profile will appear and then become obvious.

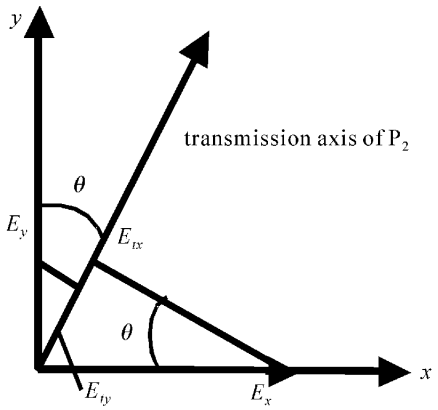

Fig. 2. Transmission of the elliptically polarized probe wave through the analyzer, uncrossed by the angle θ.

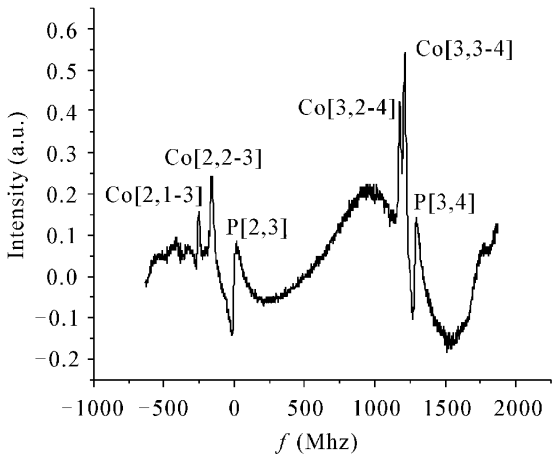

Fig. 3. The D_2 line polarization spectrum of ^{87}Rb and ^{85}Rb with $\theta = 40°$.

When $\theta = \pi/2$, the curve will turn to Lorentzian profile completely, then the spectra are similar to SAS.

Our experimental setup is shown in Fig. 1(b). Probe and pumping beams are taken from a diode laser DL100. Laser frequency is tuned to near resonant with D2 transition $F = 3 \rightarrow F = 4$ of ^{85}Rb, or $F = 2 \rightarrow F = 3$ of ^{87}Rb. Probe beam is linearly polarized with a diameter of 2 mm and power of 0.6 mW. It passes through a polarizer, a rubidium vapor cell and an analyzer, then shines to a detector. The circularly polarized pump beam caused by a $\lambda/4$ plate, with 2-mm diameter and 6.2 mW power, passes through the vapor cell inversely and overlaps with the probe beam.

The experimental result is shown in Fig. 3. The spectra P[2, 3] ($F = 2 \rightarrow F' = 3$) of ^{87}Rb and P[3, 4] ($F = 3 \rightarrow F' = 4$) of ^{85}Rb are dispersion profile. But the crossover peaks Co[2,1-3] and Co[2,2-3] of ^{87}Rb, and Co[3,2-4] and Co[3,3-4] of ^{85}Rb are Lorentzian profile.

When we change the value of θ from 0° to 45°, the dispersion peak P[2, 3] of ^{87}Rb increases gradually (see Fig. 4). If the θ changes from 45° to 90°, the dispersion intensity of P[2, 3] decreases and turns to Lorentzian profile

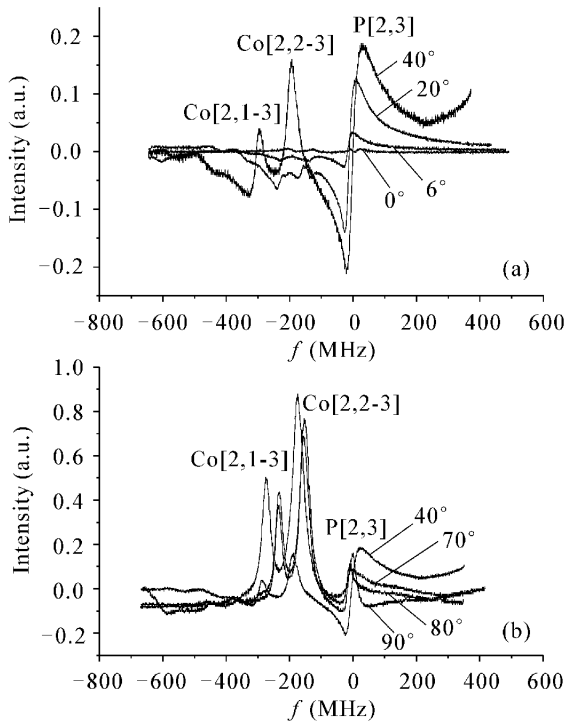

Fig. 4. The D_2 line polarization spectrum of ^{87}Rb with uncrossed angle θ.

step by step. When θ is 90°, the peak becomes Lorentzian profile, just as SAS.

We got an excellent dispersion profile at an optimistic value of θ (about 40°). It was fed back to the diode laser to stabilize its frequency. A Fabry-Perot interferometer was used to monitor the linewidth of the laser. We can narrow the laser frequency to 2 MHz in this way.

In summary, we studied the polarization spectra of rubidium atoms, and found that the experimental spectra agreed with the qualitative analysis. We also stabilized the frequency of diode laser using PS. It is found that the present technique is a more convenient and easier method for frequency stabilization than SAS. Further narrower linewidth could be reached by carefully using the method.

This work was supported by the National Natural Science Foundation of China under Grant No. 10104018. K. Jiang's e-mail address is kjjiang@wipm.ac.cn.

References

1. C. Wieman and T. W. Hänsch, Phys. Rev. Lett. **36,** 1170 (1976).
2. V. S. Letokov and V. P. Chebotayev, *Nonlinear Laser Spectroscopy, Springer Series in Optics Sciences* (Vol. 4) (Springer-Verlag, Berlin, 1977).
3. S. Nakayama, J. Phys. Soc. Jpn. **50,** 609 (1981).
4. S. Nakayama, Opt. Commun. **50,** 19 (1984).
5. J. Wang, X. J. Liu, J. M. Li, K. J. Jiang, and M. S. Zhan, Chin. J. Quantum Electron. (in Chinese) **17,** 43 (2000).
6. W. Demtröder, *Laser Spectroscopy – Basic Concepts and Instrumentation* (Springer-Verlag, Berlin, Heidelberg, 1996) p. 459.